

# Streamer propagation in the atmosphere of Titan and other N<sub>2</sub>:CH<sub>4</sub> mixtures compared to N<sub>2</sub>:O<sub>2</sub> mixtures

Christoph Köhn<sup>1\*</sup>, Saša Dujko<sup>2</sup>, Olivier Chanrion<sup>1</sup>, Torsten Neubert<sup>1</sup>

<sup>1</sup> *Technical University of Denmark, National Space Institute (DTU Space), Elektrovej 328, 2800 Kgs Lyngby, Denmark*

<sup>2</sup> *Institute of Physics, University of Belgrade, Pregrevica 118, 11080 Belgrade, Serbia*

## Abstract

Streamers, thin, ionized plasma channels, form the early stages of lightning discharges. Here we approach the study of extraterrestrial lightning by studying the formation and propagation of streamer discharges in various nitrogen-methane and nitrogen-oxygen mixtures with levels of nitrogen from 20% to 98.4%. We present the friction force and breakdown fields  $E_k$  in various N<sub>2</sub>:O<sub>2</sub> (Earth-like) and N<sub>2</sub>:CH<sub>4</sub> (Titan-like) mixtures. The strength of the friction force is larger in N<sub>2</sub>:CH<sub>4</sub> mixtures whereas the breakdown field in mixtures with methane is half as large as in mixtures with oxygen. We use a 2.5 dimensional Monte Carlo particle-in-cell code with cylindrical symmetry to simulate the development of electron avalanches from an initial electron-ion patch in ambient electric fields between  $1.5E_k$  and  $3E_k$ . We compare the electron density, the electric field, the front velocities as well as the occurrence of avalanche-to-streamer transition between mixtures with methane and with oxygen. Whereas we observe the formation of streamers in oxygen in all considered cases, we observe streamer inceptions in methane for small percentages of nitrogen or

---

\*Corresponding author: koehn@space.dtu.dk

for large electric fields only. For large percentages of nitrogen or for small fields, ionization is not efficient enough to form a streamer channel within the length of the simulation domain. In oxygen, positive and negative streamers move faster for small percentages of nitrogen. In mixtures with methane, electron or streamer fronts move 10-100 times slower than in mixtures with oxygen; the higher the percentage of methane, the faster the fronts move.

## 1 Introduction

Lightning on Earth is a highly complex phenomenon involving physical processes on various spatial and temporal scales [1, 2, 3, 4, 5, 6] starting from electron avalanches and resulting in the formation of hot, conducting lightning leaders. The early stages of lightning discharges are formed by streamers, thin, ionized plasma channels [7, 8, 9, 10, 3, 11, 12, 13]. Three necessary, yet not sufficient, conditions for the inception of streamers are the presence of initial free electrons with a sufficiently high density, a sufficiently high ambient electric field to accelerate electrons and an ambient gas as a source of new electrons to sustain the streamer discharge.

In our solar system, lightning activity has been detected on several planets. While the occurrence of lightning on Venus is still a controversial question [14, 15, 16, 17], we possess clear evidences of lightning in the atmospheres of the gas and ice giants. Since Voyager 1, every probe that has approached Jupiter has imaged lightning flashes from its night side. Lightning has also been identified on Jupiter by its very-low frequency (VLF) radio signatures [18, 19]. On Saturn, lightning has been recently detected optically and by its high-frequency (HF) radio signals [20, 21], known as Saturn electrostatic discharges (SED) [22]. HF radio signals similar to those observed on Saturn have been detected by the Voyager 2 radio instrument at Uranus [19, 23]. Lightning is also believed to take place at Neptune, based on the detection of lightning whistler like events observed during the encounter of Voyager 2 with this planet [24, 25], and on Mars, in dust storms, based on the measurements of higher order moments of the electric field by a detector installed on NASA's Deep Space Network [26, 27] and supported by simulations by [28]. However, more recent measurements on Mars by Anderson et al. [29] and by Gurnett et al. [30] using the Allen Telescope and the radar receiver of the Mars Express have not found any signatures of lightning discharges. Hence, it is still controversial whether lightning exists on Mars.

The existence of atmospheric electric discharges on these planets has been modelled by numerical simulations and tested by laboratory experiments.

Using Monte Carlo simulations, Dwyer et al. [31] simulated the runaway breakdown, which is the discharge initiation through high-energy electrons whose friction is significantly smaller than for low-energy electrons [32], in the atmospheres of Jupiter and Saturn. They found that the runaway breakdown field lowered by the presence of hydrometeors is ten times smaller than the conventional breakdown field and suggest that this might facilitate lightning inception on these planets.

Borucki et al. [33] experimentally simulated lightning discharges on Venus, Jupiter and Titan by initiating laser-induced plasmas in various gas mixtures and found that the emitted spectral lines of these induced discharges depend significantly on the gas composition. On Jupiter, they mainly observed spectral lines associated with hydrogen whilst plasmas on Titan and Venus show spectral lines related to the abundance of the carbon molecules  $\text{CH}_4$  and  $\text{CO}$ .

Dubrovín et al. [34] investigated experimentally the inception and the motion of streamer discharges in  $\text{CO}_2:\text{N}_2$  and  $\text{H}_2:\text{He}$  as they are present in the atmospheres of Venus and Jupiter in pressures between 25 and 200 mbar. They discovered that streamer discharges exist in these atmosphere, yet fainter than on Earth. However, to the best of our knowledge, there have not been any simulations of streamer discharges and their inception in non-terrestrial gas compositions modelling the very early stages of lightning discharges.

Amongst the bodies of our solar system, not only planets, but also some of their moons shelter an atmosphere, such as Jupiter's satellite Europa with a pressure of  $10^{-11}$  bar [35] or Saturn's moon Titan. Both satellites are suspected to host aminoacids [36, 37] which are a necessary condition for the formation of life as we know it [38, 39, 40]. Waite Jr. et al. [41] discussed that cosmic gamma-rays enter Titan's atmosphere and facilitate the formation of organic compounds, so-called Tholins. Its atmosphere mainly contains carbonaceous methane and nitrogen which resembles the atmosphere of the primordial Earth mainly consisting of carbon monoxide, water, methane and nitrogenous ammonia. Urey and Miller [42, 43] mimicked lightning by performing spark discharges in the same gas mixture as of primordial Earth. They discovered that aminoacids were formed in their set-up concluding that lightning could be one trigger for the formation of life. Similarly, Plankenstein et al. [44] performed discharge experiments in a gas resembling the composition on Titan and found that possible discharges can produce higher hydrocarbons and molecules relevant for the formation of amino acids and nucleic acids.

First attempts to detect lightning on Titan were executed in 1980 when Voyager 1 flew by Saturn and Titan [45]. Since the thickness of clouds and haze layers prevented the measurements of optical signatures, the search was

extended towards spherics at radio wavelengths. However, no relevant data was recorded concluding that the maximum energy of a lightning flash on Titan would be approx. 1 MJ, approx. 1000 times weaker than for lightning flashes on Earth [46].

In 2005, the Huygens Atmospheric Structure Instrument (HASI), designed to accurately measure atmospheric properties of Titan, measured a resonance at 36 Hz initially linked to the occurrence of lightning [47]. Yet, a subsequent analysis of the provided data rather suggested that this resonance is an artifact of Titan's interaction with Saturn's magnetosphere [48].

Successively, Cassini's RPWS (Radio and Plasma Wave Science) instrument [49, 50, 51, 52] tried to search for radio emissions as an indicator for lightning on Titan during, in total, 107 flybys. Again, during these missions, no positive results were found; however, the conclusion was not that lightning does not exist on Titan, but rather that, if lightning exists, it is too weak to be detected.

Despite the fact that lightning has not been observed directly by cameras on-board or indirectly by radio instruments during Cassini's observations or during the descent of the Huygens probe, the atmospheric chemistry suggests the presence of electrical discharges in the atmosphere of Titan. Titan has a substantial atmosphere consisting predominantly of nitrogen and methane with trace amounts of hydrogen, hydrogen cyanide, ethane, propane, acetylene and other hydrocarbons and nitriles. The presence of the majority of these hydrocarbons and nitriles in the atmosphere of Titan has been explained in terms of photochemistry and charged-particle chemistry models with few exceptions. Perhaps the best known example is ethylene, which is more abundant in the upper atmosphere of Titan than photochemistry models would predict [53, 54]. Borucki et al. [54] argued that the excess of ethylene in the upper Titan's atmosphere could be explained by upward diffusion of ethylene produced in the lower parts of the atmosphere by lightning. Likewise, the presence of acetylene and hydrogen cyanide with the relatively high abundances of  $(1.9 \pm 0.2) \times 10^{-6}$  and  $(1.5 \pm 0.2) \times 10^{-7}$  [55], respectively, could also be explained by the lightning induced chemistry.

Whereas Earth's surface conductivity is approximately  $10^{-14} \text{ S m}^{-1}$  [56], Molina-Cuberos et al. [57] approximated Titan's surface conductivity to range between  $10^{-15} \text{ S m}^{-1}$  and  $10^{-10} \text{ S m}^{-1}$ , thus sufficiently large to allow the generation of cloud-to-ground lightning flashes. Tokano et al. give an extensive overview of available cloud convection and charging models as well as particle charging mechanisms (see [58] and references therein). They apply a one-dimensional time-dependent thundercloud model and state that negative space charges resulting from the attachment of electrons to clouds, can temporally create electric fields of up to  $2 \text{ MV m}^{-1}$  which is sufficient to

initiate 20 km long negative cloud-to-ground lightning.

We here strive to answer the question whether streamer discharges, the pre-cursors of lightning, exist in Titan’s atmosphere. Therefore, we perform Monte Carlo particle-in-cell simulations of electron avalanches in mixtures of  $\text{N}_2:\text{CH}_4$  with different percentages of nitrogen in various electric fields and determine for which conditions the electron avalanches transition into streamer discharges. We also run simulations in  $\text{N}_2:\text{O}_2$  mixtures with the same percentage of nitrogen and compare results for methane and for oxygen.

In section 2 we briefly discuss the atmospheric profile of Titan and the set-up of our simulations. Additionally, we discuss the friction forces as well as the electric breakdown fields in different  $\text{N}_2:\text{O}_2$  and  $\text{N}_2:\text{CH}_4$  mixtures. In section 3 we discuss the temporal evolution of the electron densities, the front velocities and the resulting electric field and compare results in mixtures with methane and with oxygen. We discuss when avalanche-to-streamer transitions are feasible and relate our results to the friction force and thus to the electron energy distribution. In section 4 we summarize our results and discuss whether lightning is possible to occur on Titan. Finally, we give an outlook on future research activities.

## 2 Modelling and properties of Titan’s atmosphere

### 2.1 Set-up of the model

We simulate the development of electron avalanches and, if existent, of subsequent streamers with a 2.5D Monte Carlo Particle-In-Cell code with cylindrical symmetry with two spatial coordinates  $(r, z)$  and three coordinates  $(v_r, v_\theta, v_z)$  in velocity space for each individual (super)electron [59, 60]. We perform simulations in mixtures of  $\text{N}_2:\text{O}_2$  and of  $\text{N}_2:\text{CH}_4$  with different percentages  $\kappa$  of  $\text{N}_2$ . Thus, Earth’s atmosphere is determined by  $\kappa = 0.8$  with its nitrogen-oxygen mixture and Titan’s atmosphere by  $\kappa = 0.984$  with its nitrogen-methane mixture. For a better comparison of the results in different gas mixtures, we use a gas density of  $2.9 \cdot 10^{25} \text{ m}^{-3}$  in all mixtures (see section 2.2).

The collision of electrons with nitrogen and oxygen molecules, cross sections as well as their implementation have already been studied carefully in various publications (e.g. [61, 62, 63, 64, 59, 65, 66, 67, 68]). We have reviewed the collisions of electrons with methane molecules and the resulting friction force in section 2.3.

Accounting for space charge effects, we solve the Poisson equation in the

simulation domain with dimensions  $(L_r, L_z)=(1.25, 14)$  mm and with 150 grid points in  $r$ - and 1200 grid points in  $z$ -direction [69]. As boundary conditions, we use Neumann conditions  $\partial\phi/\partial r = 0$  for  $r = 0, L_r$ , and Dirichlet conditions for the electric potential  $\phi(r, 0) = 0$  and  $\phi(r, L_z) = \phi_{max} = E_{amb} \cdot L_z$  where  $E_{amb}$  is the ambient electric field pointing downwards. We have performed simulations in ambient fields of 1.5, 2 and 3 times the classical breakdown field  $E_k$ .

We initiate all simulations with a charge neutral electron-ion patch at the center of the simulation domain. The initial electron density is given by the Gaussian  $n_e(r, z, t = 0) = n_{e,0} \exp(-(r^2 + (z - z_0)^2)/\lambda^2)$  with  $n_{e,0} = 10^{20} \text{ m}^{-3}$  as in [70, 71, 69] and  $\lambda = 0.2$  mm centered at  $z_0 = 7$  mm.

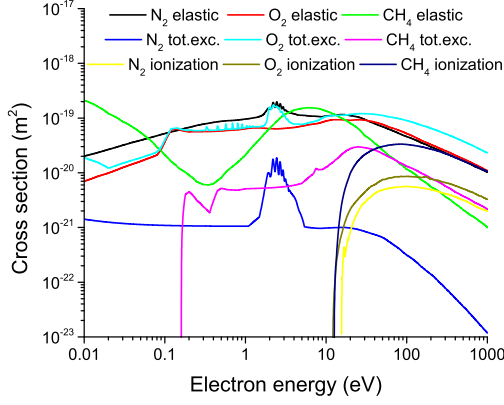
## 2.2 Titan's atmospheric composition

An overview of the abundances of the constituents of Titan's atmosphere is given in [72]. Titan's atmosphere is composed mainly of nitrogen and of methane where the percentage of methane varies from approx. 5% at ground up to approx. 1.4% at 140 km altitude. In order to perform reliable simulations, it is, however, not sufficient to know the gas composition, but we also need to specify the correct number density of ambient gas molecules. Lindal et al. and McKay et al. [73, 74] give an extended overview of Titan's temperature and pressure profile as a function of altitude. Further measurements of the temperature and pressure were later performed by the Huygens Atmospheric Structure Instrument (HASI) descending towards Titan's surface [47].

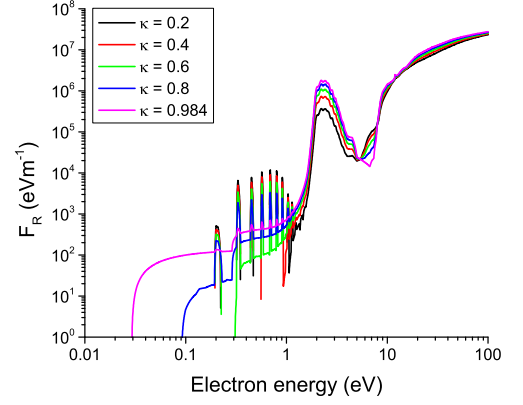
On Titan, clouds form between 20 km and 35 km altitude [75, 76] with the pressure varying between approximately 0.1 bar and 0.6 bar, the temperature varying between 70 K and 75 K and the level of methane varying between 1.6% and 2.0% [77]. Hence, we here choose 1.6% of methane as well as  $p = 0.3$  bar and  $T = 75$  K yielding a gas density of  $n_{Titan} = p/(k_B T) \approx 2.9 \cdot 10^{25} \text{ m}^{-3}$  using the ideal gas law. On Earth a density of  $2.9 \cdot 10^{25} \text{ m}^{-3}$  corresponds to a pressure of approx. 1.2 bar at 300 K or approx. 1 bar at 250 K (equivalent to 10 km altitude).

## 2.3 Cross sections and friction forces for electrons in $\text{N}_2:\text{O}_2$ and $\text{N}_2:\text{CH}_4$ mixture

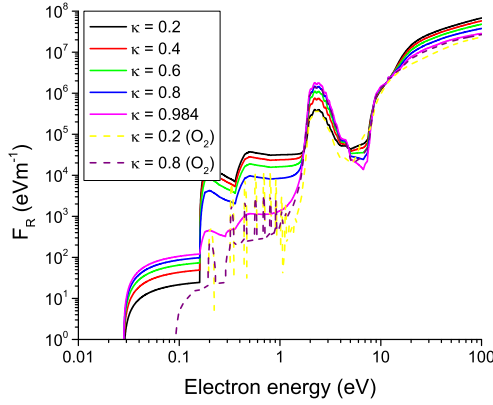
Figure 1 a) shows the cross sections  $\sigma_{i,j}$  for different collision processes  $j$  of electrons at different species  $i$ . As for oxygen, electrons scatter off methane elastically, excite, ionize or attach to it. The most frequent process below



a)  $\sigma_{i,j}$



b)  $F_R, N_2:O_2$



c)  $F_R, N_2:CH_4$

Figure 1: a) Cross sections for electron scattering in  $N_2$ ,  $O_2$  and  $CH_4$ . We show cross sections for momentum transfer in elastic collisions, total cross sections for electronic excitation (including dissociation into neutral fragments) and cross sections for electron-impact ionization. b,c) The friction force in  $N_2:O_2$  (b) and in  $N_2:CH_4$  (c) as a function of electron energy for different percentages  $\kappa$  of molecular nitrogen. For comparison, the dashed yellow and purple lines in c) show the friction force for a  $N_2:O_2$  mixture with 20% and 80% nitrogen.

approximately 50 eV is elastic scattering followed by excitations [78]. Since the ionization threshold energy is  $E_b \approx 12.6$  eV, the ionization cross section starts to increase for energies above and becomes predominant above approximately 50 eV.

However, due to the lack of reliable data, we do not have differential cross sections for elastic and inelastic collisions, including those for ionization. However, as we discuss below, most of the electrons in the  $\text{N}_2:\text{CH}_4$  simulations have energies below 50 eV. For such low energies, the collision dynamics is well described by the approximation of isotropic scattering. The isotropy of scattering may be assumed due to the fact that numerous elastic collisions generally randomize directions of electron motion and hence one could not see any significant effects of introducing the anisotropy of scattering. The determination of the momentum transfer cross section is usually performed under the assumption of anisotropy, so the cross section has this assumption inherently built into it. Of course, for higher electron energies the approximation of isotropic scattering is no more valid and the use of differential cross sections for electron scattering is mandatory (see for example a detailed discussion in [79]). The energy  $W$  of secondary ionization electrons is determined uniformly randomly in  $[0, E_{in} - E_b]$  where  $E_{in}$  is the kinetic energy of the incident electron. Subsequently, we apply the conservation of energy and momentum and determine [67, 80] the scattering angle

$$\cos \Theta_{sca} = \sqrt{\frac{(E_{in} - W)(E_{in} + 2m_e c^2)}{E_{in}(E_{in} - W + 2m_e c^2)}} \quad (1)$$

of the incident electron and the emission angle

$$\cos \Theta_e = \sqrt{\frac{W(E_{in} + 2m_e c^2)}{E_{in}(W + 2m_e c^2)}}. \quad (2)$$

of the liberated electron with  $m_e$  being the electron's rest mass and  $c$  the speed of light. Note that these relativistic equations are valid also for non-relativistic electron energies.

Figure 1 b,c) show the friction force

$$F_R(E) = \sum_{i,j} n_i \sigma_{i,j}(E) \Delta E_{i,j}, \quad (3)$$

where  $n_i$  is the partial density [ $\text{m}^{-3}$ ] of  $\text{N}_2$ ,  $\text{O}_2$  or  $\text{CH}_4$ ,  $\sigma_{i,j}$  is the total cross section for collision process  $j$  of electrons at molecule species  $i$  and  $\Delta E_{i,j}$  the respective energy loss of electrons. The sum is taken over all involved

molecule species  $i$  and over all involved inelastic collisions  $j$ . Note that excitations and ionization are the only processes below 100 eV contributing to the friction where the energy loss resulting from excitations is the threshold energy of the collision and the energy loss for ionization is  $1/2(E_{in} - E_b)$ . Panel b) shows the friction of electrons in different mixtures of  $N_2:O_2$ . The overall shape is similar irrespective of the percentage  $\kappa$  of nitrogen. However, the strength of excitational losses for energies below 1 eV increases with decreasing  $\kappa$  since the cross section and subsequently the contribution of excitations is higher for oxygen than for nitrogen. On the contrary, the contribution of excitations above 1 eV increases with increasing percentage of nitrogen. For  $E \gtrsim 1$  eV, there is a resonance in the cross section of the vibrational states of excited nitrogen with threshold energies of approximately 2 eV (see for example Tab. 1 in [64]). For energies above approximately 10 eV, the friction forces for different  $\kappa$  align because the total ionization cross section and the corresponding energy loss are comparable for nitrogen and oxygen.

Panel c) shows the friction force for different  $N_2:CH_4$  mixtures. For comparison, the yellow and purple lines additionally show the friction force for  $N_2:O_2$  with 20% and 80% nitrogen. Whilst the overall shape of the friction force is different than for  $N_2:O_2$ , we observe the same dependency on  $\kappa$ : Since the cross section for exciting methane for electron energies below 1 eV is larger than for nitrogen, the friction force increases for an increasing percentage of methane. Because of the resonance of the cross section for exciting nitrogen above 1 eV, the friction increases with  $\kappa$  for energies between 1 eV and 10 eV. Comparing the friction force in  $N_2:O_2$  mixtures with the friction force in  $N_2:CH_4$  mixtures reveals that, for fixed  $\kappa$ , the strength of the friction force above approximately 1 eV is similar for mixtures with oxygen and with methane, hence the energy loss of electrons above 1 eV is comparable. However, it is noticeable that for energies below 1 eV and fixed  $\kappa$ , the friction in  $N_2:CH_4$  mixtures is approximately one to two orders of magnitude higher than in mixtures with oxygen.

## 2.4 Photoionization

In oxygen-nitrogen mixtures, one additional process contributing to the evolution of streamer discharges is photoionization: Electrons can excite nitrogen which subsequently emits UV photons. In return, these UV photons ionize oxygen and thus deliver a new source of electrons [81, 82, 83, 84, 69]. Although this process is not crucial for the development for negative fronts, it supports their motion (see e.g. a discussion in [82, 69]). For positive streamer fronts moving towards the cathode, however, photoionization is one of the

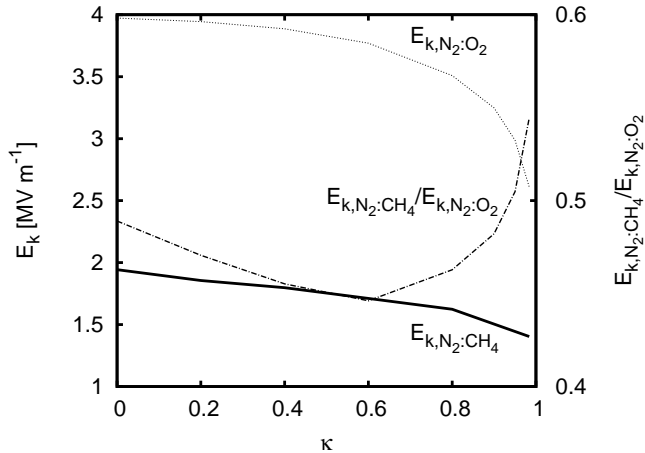


Figure 2: The breakdown field  $E_k$  as a function of the percentage  $\kappa$  of nitrogen in  $N_2:O_2$  mixtures and in  $N_2:CH_4$  mixtures with a gas density of  $2.9 \cdot 10^{25} \text{ m}^{-3}$ . The plot also shows the ratio of the breakdown fields between these two different mixtures (right  $y$ -axis).

key drivers next to background ionization [85, 86].

In oxygen, we use the model of Zheleznyak et al. [81, 59, 69] which relates the number of UV photons with energies between 12.10 eV and 12.65 eV to the number of electron impact ionization. This is the energy range where photons do not interact with nitrogen and predominantly ionize molecular oxygen. Beyond 12.65 eV, photons mainly excite nitrogen and do not contribute to the ionization of oxygen anymore [12, 87]. The ionization energy of molecular nitrogen is 15.6 eV, thus larger than the upper limit for UV photoionization. Note that the threshold energy for the ionization of oxygen is 12.1 eV, thus on the lower limit of the energy of considered UV photons.

Since the ionization energy of methane is 12.6 eV, photoionization by UV photons still contributes to the development of electron avalanches or streamers in  $N_2:CH_4$ , even though less efficiently. We thus implement the model of Zheleznyak et al., but evaluate the UV photoionization process randomly in  $(12.65-12.6)/(12.65-12.1)=9\%$  of all photoionization events in the model by Zheleznyak et al. only which is the ratio of the energy intervals of UV photoionization in methane and in oxygen.

## 2.5 The electric breakdown field

During the motion of electrons through ambient gas, electrons undergo two competing processes: First, they gain energy through the background electric

field and they lose energy through inelastic collisions with the ambient gas molecules. Second, amongst these inelastic collisions, electrons are capable of ionizing the ambient gas and multiply the total electron number as long as the primary electron's energy is above the ionization threshold energy. As a competing process, electrons attach to molecules reducing the total electron number. These two processes compete with each other and severely depend on the ambient electric field [88]. The breakdown (or equilibrium) field  $E_k$  is defined as the electric field when these two processes are in equilibrium, i.e. the rate of attachment equals the rate of ionization. Thus, in order to initiate and sustain an electron avalanche and eventually transition into a streamer, electric fields at least above the breakdown field are required such that there is a sufficient number of ionization events.

In an accompanying paper, we have determined swarm parameters like the ionization coefficients and the breakdown field for various mixtures of  $\text{N}_2:\text{O}_2$  and  $\text{N}_2:\text{CH}_4$  by applying a multi-term approach for solving the Boltzmann equation [89]. Figure 2 shows the breakdown field as a function of the percentage  $\kappa$  of nitrogen for a density of  $2.9 \cdot 10^{25} \text{ m}^{-3}$  as well as the ratio between the breakdown fields in  $\text{N}_2:\text{O}_2$  and  $\text{N}_2:\text{CH}_4$ . It shows that in both gas mixtures, the breakdown field slightly decreases as a function of  $\kappa$ . It also shows that the ratio of the breakdown field in  $\text{N}_2:\text{O}_2$  and in  $\text{N}_2:\text{CH}_4$  is approximately 0.5 irrespective of  $\kappa$  although increasing for large  $\kappa$ . Whilst the electric field strength for breakdown varies between 3 and 4  $\text{MV m}^{-1}$  in  $\text{N}_2:\text{O}_2$ , it amounts to only 1.5-2  $\text{MV m}^{-1}$  in  $\text{N}_2:\text{CH}_4$  mixtures.

## 3 Results

### 3.1 Temporal evolution of electron avalanches and streamers for different percentages of nitrogen

Under the influence of the ambient field the initial electron-ion patch first develops into an electron avalanche and eventually into a bidirectional streamer. The ambient electric field points downwards such that the negative front moves upwards whilst the positive front moves downwards. The attached video files show the temporal evolution of the electron density and the electric field for the gas mixtures with 20% and 1.6% methane.

Figure 3 shows the electron density and the electric field (third column) for gas mixtures with 80% nitrogen in ambient fields of  $1.5E_k$  (first row),  $2E_k$  (second row),  $3E_k$  (third row), where  $E_k$  is  $\approx 3.5 \text{ MV m}^{-1}$  in mixtures with oxygen and  $\approx 1.6 \text{ MV m}^{-1}$  in mixtures with methane, after different time steps. In columns one to three, the left halves of each panel show the electron

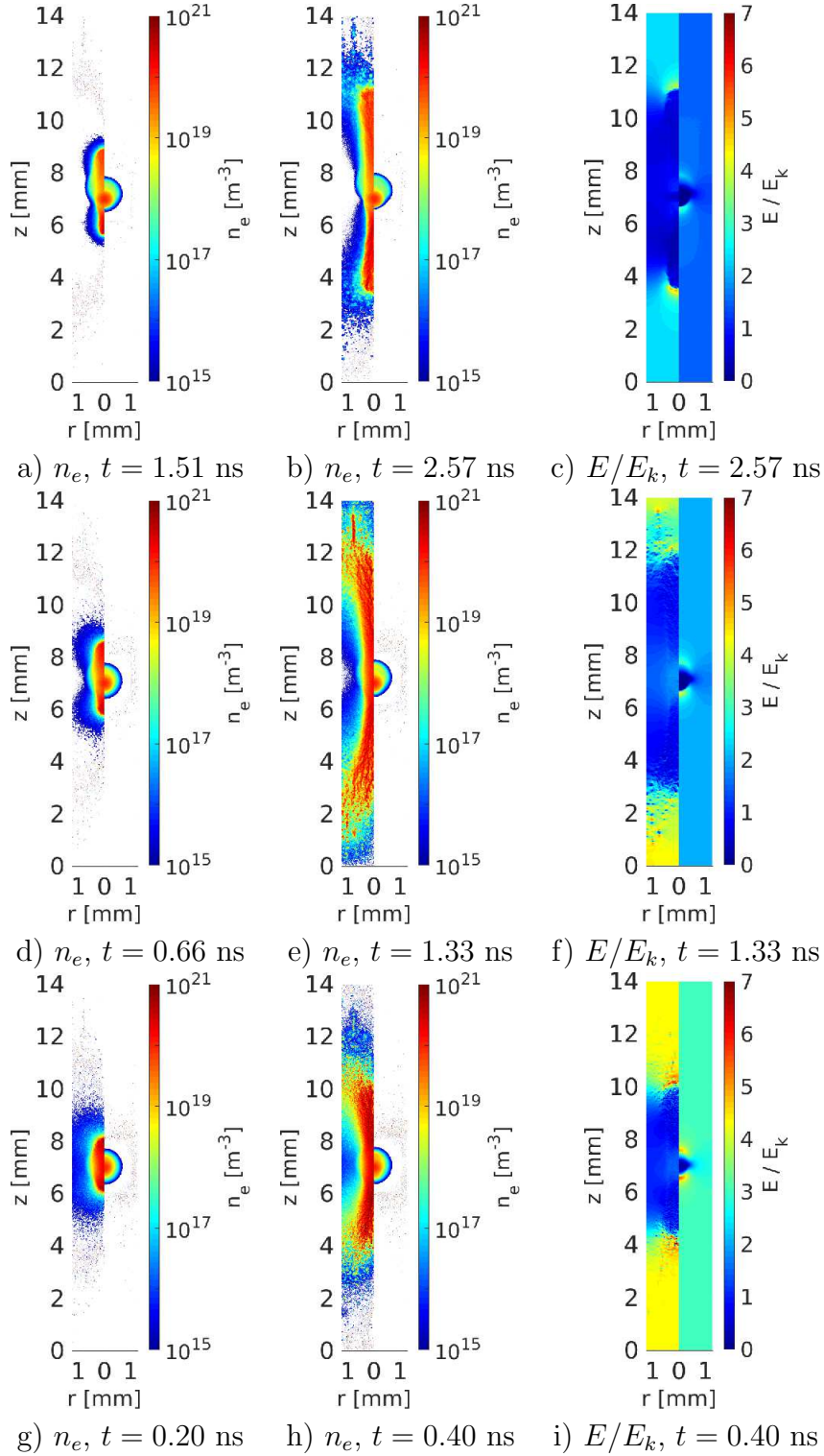


Figure 3: The electron density  $n_e$  and the electric field  $E/E_k$  in the gas mixtures  $N_2:O_2$  and  $N_2:CH_4$  with 80% nitrogen in an ambient field of  $1.5E_k$  (first row),  $2E_k$  (second row) and  $3E_k$  (third row). Columns 1 and 2 compare the electron density in mixtures with 20% oxygen (left half of each panel) with the density in mixtures with 20% methane (right half). Column 3 compares the electric field.

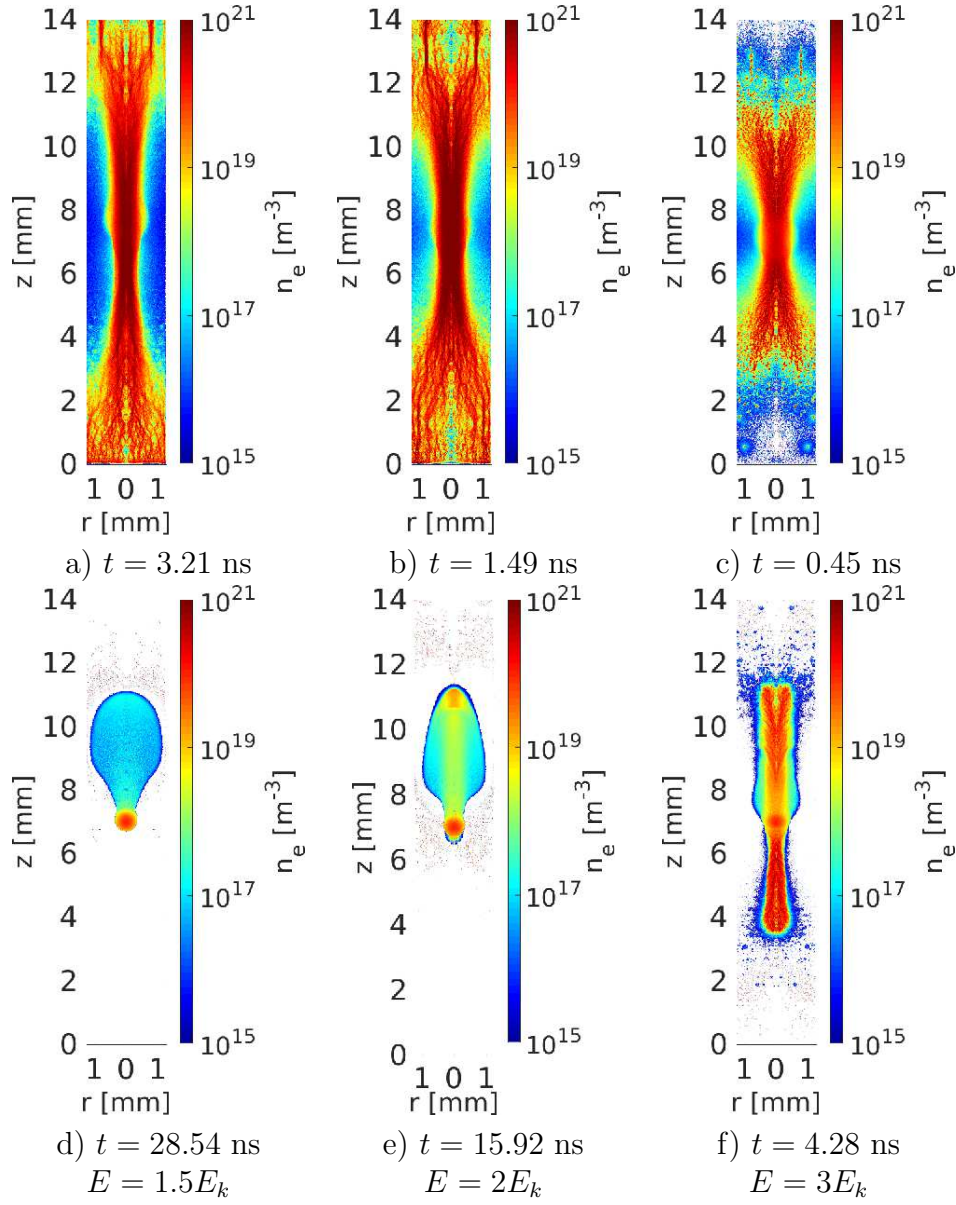


Figure 4: The electron density  $n_e$  in  $\text{N}_2:\text{O}_2$  (first row) and in  $\text{N}_2:\text{CH}_4$  (second row) with 80% nitrogen in different ambient fields at the end of the simulations.

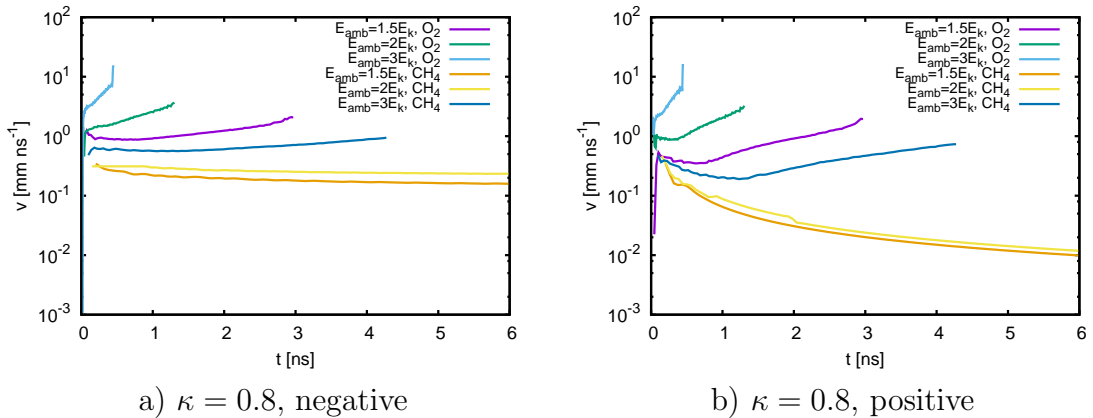
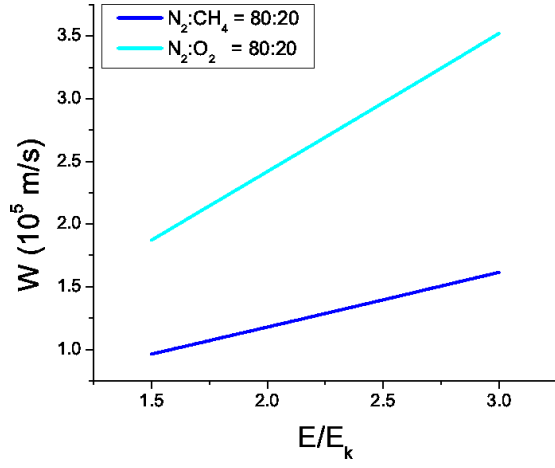


Figure 5: The velocity of the positive (first column) and negative front (second column) as a function of time for gas mixtures with 80% nitrogen.

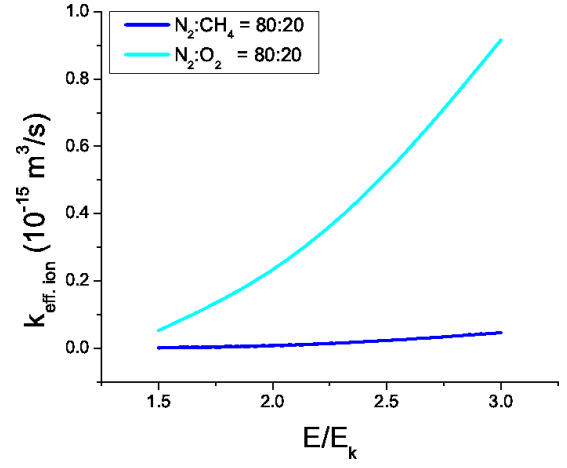
density or electric field in mixtures with 20% oxygen, i.e. the concentration on Earth whereas the right halves show the density and field in mixtures with 20% methane which we refer to as Earth-like Titan. Figure 4 shows the electron density on Earth and in Earth-like Titan mixtures at the end of our simulations.

In our simulations, the electron-ion patch on Earth develops into a bidirectional streamer for any field above  $1.5E_k$ . The electric field shows the typical streamer-like pattern with an enhanced field at the tips and a shielded field inside the streamer body. Exchanging oxygen with methane dramatically changes the picture; the process of forming electron avalanches or eventually streamers becomes delayed significantly irrespective of the applied field. Columns one and two show that there is hardly any development whilst in mixtures with oxygen, streamers have already formed after the same time steps. However, the electric field shows the same pattern as in  $N_2:O_2$  with an enhanced field at the tips of the electron patch and a vanishing shield in the patch's interior.

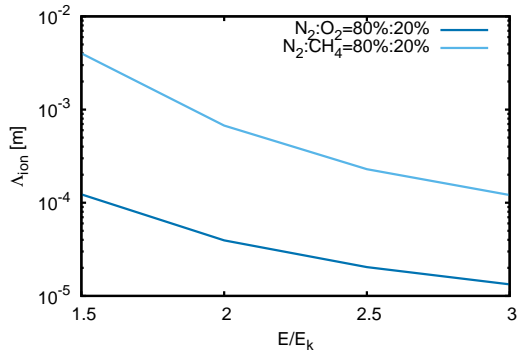
At the end of the simulations we observe three different scenarios in mixtures with  $CH_4$  depending on the ambient electric field. In a field of  $1.5E_k$ , the field at the positive front increases; however, the positive front does not move, hence there is no development of a positive streamer front. On the negative side, an electron avalanche, but no streamer front forms, without any significant field increase at the top. At the end of the simulation, the field at the tip is  $1.8E_k$  and the electron density is  $\lesssim 10^{17} \text{ m}^{-3}$ . In an ambient field of  $2E_k$ , the situation does not change significantly at the positive front. The field increases, but the front does not develop. On the negative



a)



b)



c)

Figure 6: The drift velocity (a), the effective ionization coefficient (b) and the ionization length  $\Lambda_{\text{ion}}$  (c) as a function of the ratio of the applied electric field and breakdown field.

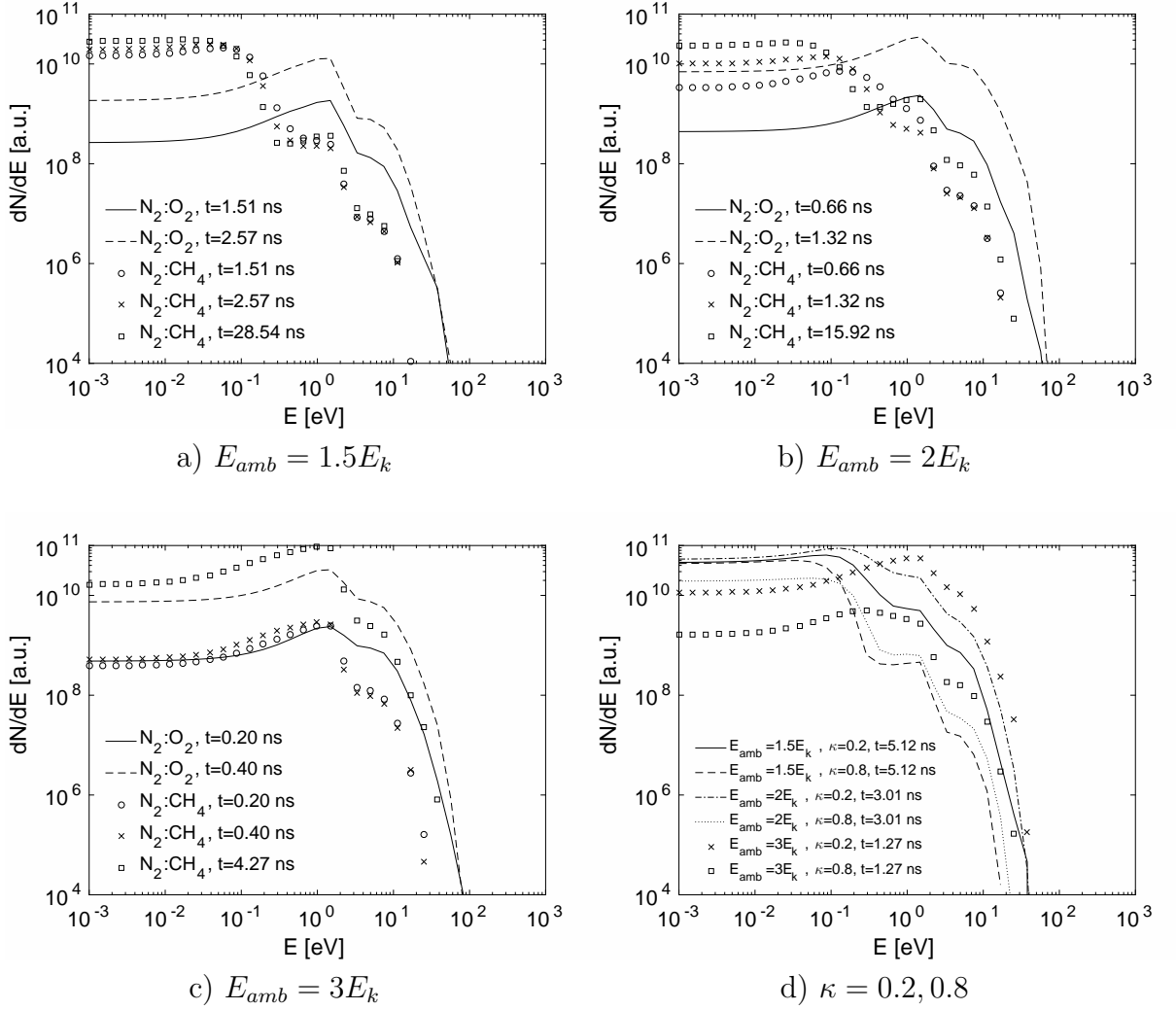
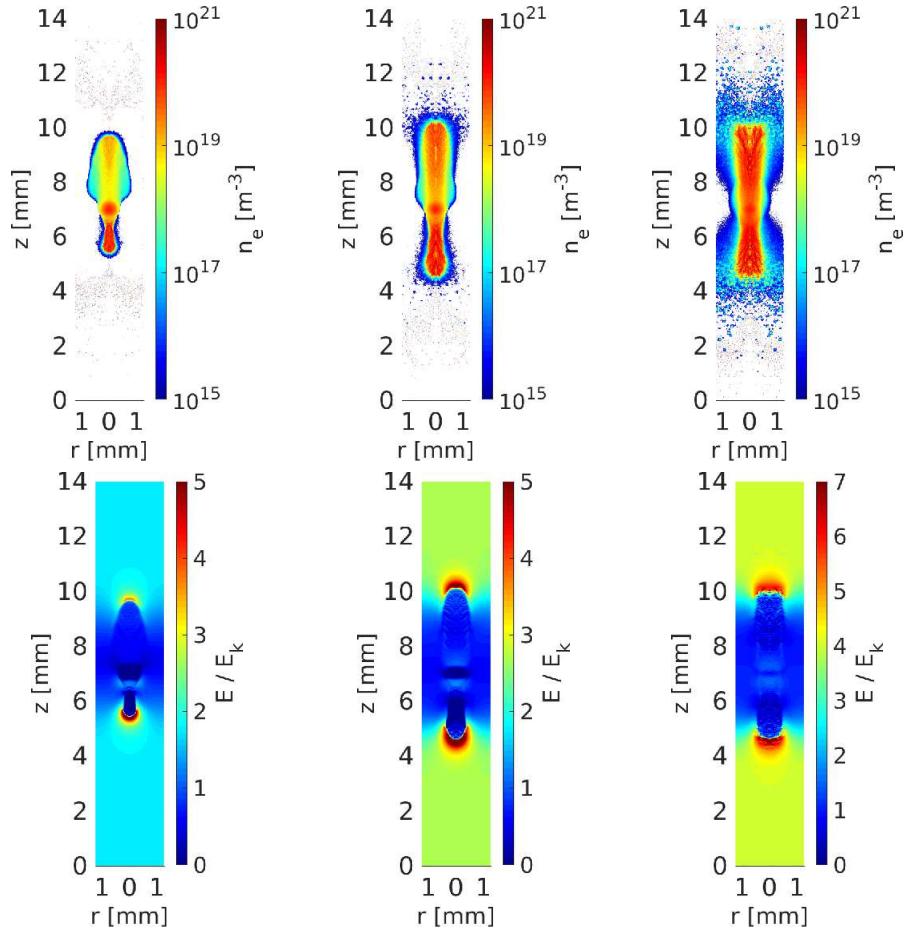


Figure 7: The electron energy distribution in an ambient field of a)  $1.5E_k$ , b)  $2E_k$  and c)  $3E_k$  for  $\kappa = 0.8$  after the same time steps as in Fig. 3. d) The energy distribution for  $\kappa = 0.2$  and for  $\kappa = 0.8$  for the same fields and time steps as in Fig. 8.



$$E = 1.5E_k, t = 5.12 \text{ ns} \quad E = 2E_k, t = 3.01 \text{ ns} \quad E = 3E_k, t = 1.27 \text{ ns}$$

Figure 8: The electron density (first row) and the electric field (second row) in  $\text{N}_2:\text{CH}_4=(20\%):(80\%)$  in different electric fields after different time steps.

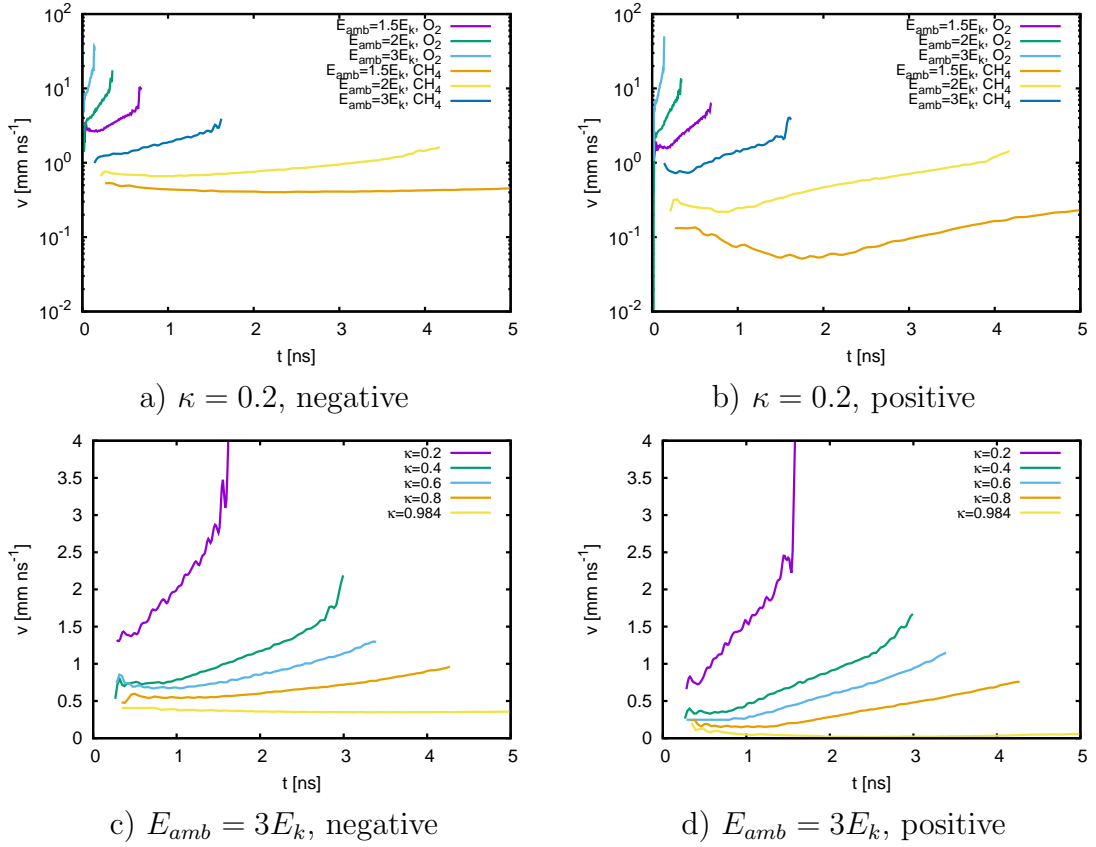


Figure 9: a,b) The velocity of the negative (a) and positive front (b) as a function of time for gas mixtures with 20% nitrogen. c,d) The velocity of the negative and of the positive front in  $N_2:CH_4$  in an ambient field of  $3E_k$  for different percentages of nitrogen.

front, however, we observe the formation of a streamer-like channel. During the simulation, the field at the tip varies between approximately  $3E_k$  and  $6E_k$  whereas the field is shielded in its interior. In contrast to the density in  $1.5E_k$  (d), the electron number slightly multiplies and reaches a density of  $\approx 10^{19} \text{ m}^{-3}$  after 15.92 ns. In  $E_{amb} = 3E_k$ , there is the distinct formation of a positive and of a negative streamer front similar to as in air. Since the breakdown fields in  $\text{N}_2:\text{O}_2$  and in  $\text{N}_2:\text{CH}_4$  differ by a factor of  $\approx 2$ , the absolute value of  $3E_k$  in  $\text{N}_2:\text{CH}_4$  corresponds to the value of  $1.5E_k$  in air. Hence, the evolution of the electron density and of the electric field is comparable although delayed.

Figure 5 shows the front velocities in the early stages of the evolution of electron avalanches and streamers for  $\kappa = 0.8$  for  $\text{O}_2$  and  $\text{CH}_4$  and for all considered electric fields. Depending on the electric field, the streamer velocity in  $\text{N}_2:\text{O}_2$  lies between  $10^0$  and  $10^1 \text{ mm ns}^{-1}$  and is similar for the positive and the negative streamer front. For  $E_{amb} = 1.5E_k$  and  $E_{amb} = 2E_k$  in  $\text{N}_2:\text{CH}_4$  the velocity of the positive front lies between  $10^{-2}$  and  $10^{-1} \text{ mm ns}^{-1}$  and is decreasing with time which is in agreement with Figures 3 d) and h) with no distinct fronts for these fields, similarly for negative fronts. For  $3E_k$ , Fig. 3 l) shows the development of a positive and a negative streamer front. The slope of the velocity is comparable to the increase of streamer velocities in air in a field of  $1.5E_k$ ; however, in air, positive fronts and negative fronts are faster than in  $\text{N}_2:\text{CH}_4$ . The delayed motion of fronts in mixtures with methane is related to the drift of electrons. Fig. 6 a) shows the drift velocity of electrons in nitrogen-methane and nitrogen-oxygen mixtures as a function of the ambient field. It is higher and increasing more significantly in mixtures with oxygen. Consequently the motion of fronts in  $\text{N}_2:\text{CH}_4$  mixtures is delayed.

The differences in the avalanche-to-streamer transition as well as in the streamer evolution between Earth and Earth-like Titan for the same  $E_{amb}/E_k$  results from different ionization lengths in  $\text{N}_2:\text{O}_2$  and in  $\text{N}_2:\text{CH}_4$  as well as from the reduced probability for photoionization. Figure 6 b) shows the effective ionization coefficient as a function of the electric field. It shows that ionization in a mixture with 20% methane is less effective than in a mixture with 20% oxygen for all considered field strengths. Beyond, the growth of the ionization coefficient is much less dominant in  $\text{N}_2:\text{CH}_4$  mixtures than in  $\text{N}_2:\text{O}_2$ . Panel c) shows the ionization length  $\Lambda_{ion}$  as a function of  $E/E_k$ . In  $\text{N}_2:\text{O}_2$  mixtures the ionization length varies from approximately 0.1 mm for  $1.5E_k$  to 0.01 mm for  $3E_k$  whilst it amounts to 4 mm for  $1.5E_k$  in  $\text{N}_2:\text{CH}_4$  mixtures with 80% nitrogen. Hence, in  $1.5E_k$  in mixtures with methane, the ionization length is comparable to the size of the simulation domain preventing the occurrence of a significant amount of ionization. Since ionization is

less effective in mixtures with methane, the build-up of space charges and thus the formation of enhanced electric field tips is delayed which reduces the electron energies and the further drive of ionization. Note that the ionization coefficient and the ionization length for  $3E_k$  in  $\text{N}_2:\text{CH}_4$  is comparable to the ionization coefficient for  $1.5E_k$  in  $\text{N}_2:\text{O}_2$ . For the same time steps and fields as in Fig. 3, Figure 7 a)-c) show the electron energy distribution. The solid and dashed lines show the typical streamer-like energy distributions of electrons in air [59] with maximum energies of  $\approx 50$  eV ( $1.5E_k$ , a),  $\approx 65$  eV ( $2E_k$ , b) and  $\approx 80$  eV ( $3E_k$ , c). However, for the same  $E_{amb}/E_k$  (remember that  $E_k$  is smaller in mixtures with methane), the maximum electron energies in  $\text{N}_2:\text{CH}_4$  are  $\approx 15$  eV (a),  $\approx 20$  eV (b) and  $\approx 30$  eV (c), thus only a little above the ionization energy of nitrogen (15.6 eV) and of methane (12.6 eV). Hence, the ionization is not effective enough to create high field tips to accelerate electrons into the energy regime where they can further create a substantial electron multiplication. Comparing the electron numbers below 1 eV in  $\text{N}_2:\text{CH}_4$  reveals that in an ambient field of  $1.5E_k$  the electron number does not change significantly because of inefficient ionization whereas the electron number increases significantly in a field of  $3E_k$ .

Figure 8 shows the electron density and electric field in  $\text{N}_2:\text{CH}_4$  with 20% nitrogen. It shows that in all considered cases negative and positive streamer fronts form. Fig. 7 d) compares the electron energy distribution for  $\kappa = 0.2$  and  $\kappa = 0.8$  for the same fields and time steps as in Fig 8. It shows that in all cases, the maximum electron energy is larger for  $\kappa = 0.2$  than for  $\kappa = 0.8$  which results from the dependence of the friction force on the percentage of nitrogen. Figure 1 b) shows that the friction force in  $\text{N}_2:\text{CH}_4$  has a resonance at approximately 2 eV enhanced for  $\kappa = 0.8$ , reducing the electron energies. Consequently, since the electron energies are larger for  $\kappa = 0.2$ , the ionization of the ambient gas as well as photoionization are more probable and the avalanche-to-streamer transition is facilitated.

For  $\kappa = 0.2$ , Figure 9 a) and b) show the streamer velocities in  $\text{N}_2:\text{O}_2$  and  $\text{N}_2:\text{CH}_4$  for all considered electric fields as a function of time. Although there is an avalanche-to-streamer transition for all field strengths, streamers move faster in oxygen than in methane. As for  $\kappa = 0.8$ , the streamer velocities equal  $\approx 10^0 - 10^1$  mm ns<sup>-1</sup> in oxygen whilst they lie between  $10^{-1}$  and approximately  $10^0$  mm ns<sup>-1</sup> in the nitrogen-methane mixture. Panels c) and d) additionally show the front velocities in  $\text{N}_2:\text{CH}_4$  in an ambient field of  $3E_k$  for different percentages of nitrogen. They illustrate that both positive and negative fronts move faster in mixtures with a low percentage of nitrogen or equivalently with a significant contribution of methane. Since the breakdown electric field does not vary much as a function of  $\kappa$ , we explain this with the friction force and its dependency on  $\kappa$ . As we have discussed in section 2.3,

the friction force has a resonance at an electron energy of approx. 2 eV which is distinct for large percentages of nitrogen. Subsequently, electron energies are lower and the fronts move slower in mixtures with high percentages of nitrogen. Equivalently fronts move substantially faster in mixtures with a significant concentration of methane.

### 3.2 The inception of streamers on Titan

After comparing the inception and evolution of bidirectional streamers in different  $\text{N}_2:\text{CH}_4$  and  $\text{N}_2:\text{O}_2$  mixtures, we now focus on the evolution of plasma patches and their transition to bidirectional streamers on Saturn’s moon Titan, hence in  $\text{N}_2:\text{CH}_4$  with 98.4% nitrogen. Figure 10 shows the electron density and the electric field in different ambient fields; we here would like to remind the reader that the number density of ambient molecules is  $2.9 \cdot 10^{25} \text{ m}^{-3}$  which corresponds to 20 km altitude on Titan, i.e. typical cloud altitudes in its atmosphere. As supplementary material, we have added movie files displaying the temporal evolution of the electron density and the electric field for the cases presented in Fig. 10. For comparison, the last column shows the electron density and the electric field in  $\text{N}_2:\text{O}_2$  for the same number density of ambient gas molecules. Similar to  $\kappa = 0.8$ , we observe the avalanche-to-streamer transition in  $\text{N}_2:\text{CH}_4$  only for fields above  $2E_k$ . As for  $\kappa = 0.8$ , the ionization length in fields below  $2E_k$  is longer in mixtures with methane, thus the ionization is delayed and subsequently also the formation of enhanced field tips. In fields  $\leq 2E_k$ , there is a distinct motion of electrons towards the positive electrode only; there is no motion of the positive front at all. However, the field is enhanced at the positive front and shielded at the negative front. Figure 11 shows the electron energies after the same time steps and in the same electric fields as in Fig. 10. The maximum electron energy is approximately 20 eV for fields smaller than  $2E_k$  in  $\text{N}_2:\text{CH}_4$ , thus there is no efficient drive of ionization.

For fields above  $2E_k$ , we observe an avalanche-to-streamer transition within the borders of the simulation domain. However, comparing the evolution on Titan (third column) and in  $\text{N}_2:\text{O}_2$  (fourth column), reveals that both streamer fronts move significantly slower in Titan’s atmosphere. Additionally, the electron density in  $\text{N}_2:\text{CH}_4$  is smaller and branching is favored. The dot-dashed and dotted lines in Figure 11 compare the electron energies for these two cases. There is a significant number of electrons above 20 eV resulting in more electron impact ionization. However, as a consequence of the friction force, the number of electrons above 20 eV is amplified in  $\text{N}_2:\text{O}_2$  in comparison to  $\text{N}_2:\text{CH}_4$  which accelerates the formation of a double-headed streamer. Furthermore, the less probable photoionization in  $\text{N}_2:\text{CH}_4$  addi-

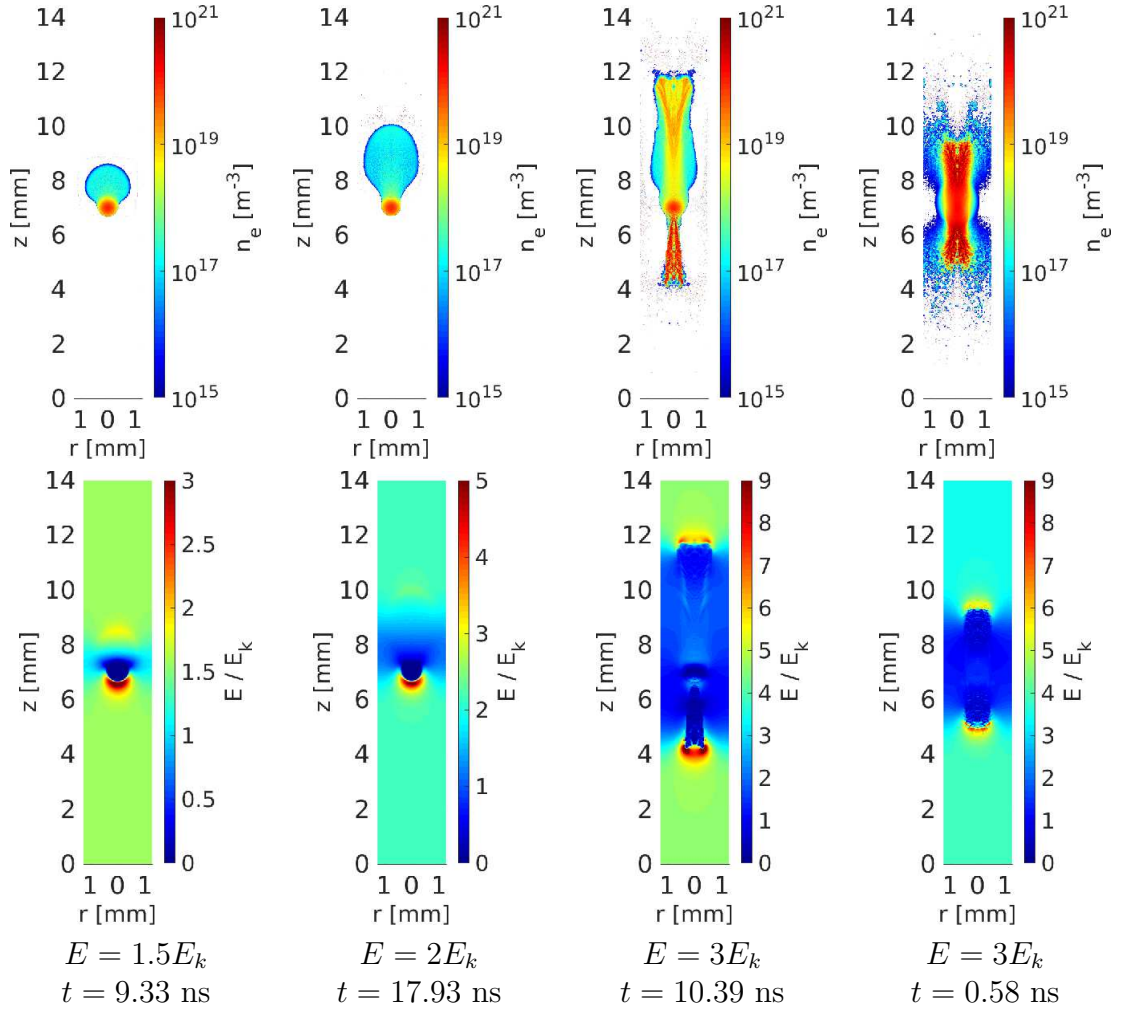


Figure 10: The electron density (first row) and the electric field (second row) in  $\text{N}_2:\text{CH}_4=(98.4\%):(1.6\%)$  (columns one to three) and in  $\text{N}_2:\text{O}_2=(98.4\%):(1.6\%)$  (fourth column) in different ambient fields after different time steps.

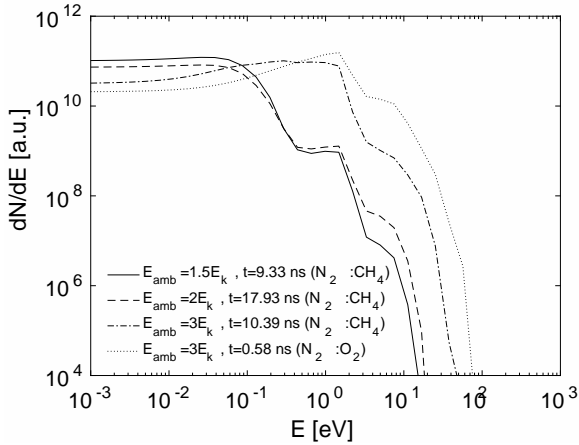


Figure 11: The energy distribution for  $\kappa = 0.984$  for the same fields and time steps as in Fig. 10.

$\kappa \backslash E_{amb}$	$1.5E_k$	$2E_k$	$3E_k$
20%	✓	✓	✓
40%		✓	✓
60%		✓	✓
80%			✓
98.4%			✓

Table 1: Criteria of successful avalanche-to-streamer transitions and subsequent streamer inception within the simulation domain with  $L_z = 1.4$  cm in nitrogen-methane mixtures with different percentages  $\kappa$  of nitrogen in different ambient fields  $E_{amb}$ .

tionally delays the streamer development.

## 4 Conclusions and outlook

We have investigated the motion of electrons and the streamer inception in  $N_2:CH_4$  and in  $N_2:O_2$  mixtures with number densities of  $2.9 \cdot 10^{25} \text{ m}^{-3}$  with different percentages  $\kappa$  of nitrogen in ambient fields of  $1.5E_k$ ,  $2E_k$  and  $3E_k$ . Whilst streamers form for all considered cases in  $N_2:O_2$ , we observe the streamer inception in  $N_2:CH_4$  mixtures depending on  $\kappa$  and the ambient field  $E_{amb}$ . Table 1 shows which combinations of  $\kappa$  and  $E_{amb}$  favor the formation of double-headed streamers in  $N_2:CH_4$  within the simulation domain. There are two scenarios: For small percentages of nitrogen, fields as low as  $1.5E_k$  are

sufficient to incept streamers; if the percentage of nitrogen is increased, higher and higher fields are required. Using a 1.5D fluid model, we have observed the same tendency for negative streamers irrespective of the initial electron density [89]. Ambient fields slightly above the breakdown field, where the rate of ionization is higher than the rate for attachment, the effective ionization coefficient for large  $\kappa$  is not sufficient to effectively ionize the ambient gas within the simulation domain. For large percentages of nitrogen and small fields, the ionization length can be larger than or comparable to the size of the simulation domain preventing us from observing the inception of streamers.

Considering that for all  $\kappa$ , the breakdown field in  $\text{N}_2:\text{CH}_4$  is approximately half as large as the breakdown field in  $\text{N}_2:\text{O}_2$  and that the friction force below 3 eV is larger in  $\text{N}_2:\text{CH}_4$ , fronts move one to two orders of magnitude faster in nitrogen-oxygen mixtures than in nitrogen-methane mixtures independent of whether we observe an avalanche-to-streamer transition. As an additional effect, photoionization is less effective in  $\text{N}_2:\text{CH}_4$ , hence, the motion of the fronts is further damped.

On Titan with methane percentages between 1.4% and 5%, we do not observe any streamer inception for ambient fields below  $\approx 3E_k$  which equals a field strength of  $4.2 \text{ MV m}^{-1}$ . Recent simulations have calculated large scale electric fields as high as  $2 \text{ MV m}^{-1}$  in Titan's atmosphere [58]. Thus, at first glance it seems that streamer inception is not feasible in Titan's atmosphere. However, one may not forget that typical large scale electric fields in Earth's thunderclouds are typically in the order of  $0.1\text{-}0.2 \text{ MV m}^{-1}$  [90, 91] whereas the classical breakdown fields at cloud altitudes vary between approximately  $2.0 \text{ MV m}^{-1}$  at 4 km altitude and  $0.5 \text{ MV m}^{-1}$  at 16 km altitude, thus approximately an order of magnitude larger. Although the origin of lightning on Earth is still under debate [92, 93], its existence, and thus also streamer inception, are very well observed despite the difference between the large-scale thundercloud fields and the breakdown field. However, we note that the inception of streamers in Titan's atmosphere strongly depends on the ambient field which is still uncertain since it is only provided by models, but not by direct measurements. Moreover, even if we conclude the existence of small (cm-long) streamer discharges in Titan's atmosphere, this does not allow us to conclude about the existence of lightning. Although their existence cannot be ruled out completely, 127 flybys of Cassini did not reveal any traces of lightning [94]. Thus, either lightning was too weak to be detected [52, 94], or it was not present at all. Since even on Earth, the streamer-to-lightning-leader transition is not fully understood yet [6], we propose further work to study this transition in Titan's atmosphere.

Since the primordial atmosphere of Earth had a similar chemical composition as Titan's atmosphere, our model here allows us to also study the

inception of streamers on the early Earth.

We here speculate that similar to the processes in terrestrial streamer discharges, run-away electrons and subsequently X-rays might be produced in Titan's atmosphere. In future work, we will estimate the occurrence and the fluence of these phenomena related to Titan  $\gamma$ -ray flashes (TGRFs) and discuss their effect on Titan's atmosphere.

The model presented in this manuscript also allows to study the streamer inception in different atmospheres, as for example, of exoplanets [95, 96, 97], provided appropriate cross sections for the scattering of electrons off the atmospheres' constituents are known. Hence, in future work, we strive to investigate which known exoplanets are likely to show discharge phenomena and also tackle the question of associated high-energy beams.

**Acknowledgments:** We would like to thank Georg Fischer from the Institut für Weltraumforschung (IWF), Graz, Austria, for fruitful discussions to improve the paper. The research was partly funded by the Marie Curie Actions of the European Union's Seventh Framework Programme (FP7/2007-2013) under REA grant agreement n° 609405 (COFUNDPostdocDTU). This project has received funding from the European Union's Horizon 2020 research and innovation programme under the Marie Skłodowska-Curie grant agreement 722337. SD acknowledges support from MPNTRRS Projects OI171037 and III41011.

## References

- [1] Y. Villanueva, V.A. Rakov, M.A. Uman, M. Brook, 1994. Microsecond-scale electric field pulses in cloud lightning discharges. *J. Geophys. Res.*, vol. 99, pp. 14353–14360
- [2] U. Ebert, C. Montijn, T.M.P. Briels, W. Hundsdorfer, B. Meulenbroek, A. Rocco and E.M. van Veldhuizen, 2006. The multiscale nature of streamers. *Plasma Sour. Sci. Technol.*, vol. 15, pp. 118–119
- [3] U. Ebert and D.D. Sentman, 2008. Streamers, sprites, leaders, lightning: from micro- to macroscales. *J. Phys. D: Appl. Phys.*, vol. 41, 230301
- [4] A. Luque and U. Ebert, 2012. Density models for streamer discharges: beyond cylindrical symmetry and homogeneous media. *J. Comp. Phys.*, vol. 231, pp. 904–918
- [5] V.A. Rakov, 2013. The Physics of Lightning. *Surv. Geophys.*, vol. 34, pp. 701–729
- [6] C.L. da Silva and V.P. Pasko, 2013. Dynamics of streamer-to-leader transition at reduced air densities and its implications for propagation of lightning leaders and gigantic jets. *J. Geophys. Res.*, vol. 118, 13561
- [7] L.B. Loeb, 1939. *Fundamental Processes of Electrical Discharges in Gases*. Wiley, New York.
- [8] H. Raether, 1939. Die Entwicklung der Elektronen in den Funkenkanal. *Z. für Phys.*, vol. 112, pp. 464-489
- [9] L.B. Loeb and J.M. Meek, 1940. The mechanism of spark discharge in air at atmospheric pressure. *J. Appl. Phys.*, vol. 11, pp. 438-447
- [10] R. Morrow and J.J. Lowke, 1997. Streamer propagation in air. *J. Phys. D: Appl. Phys.*, vol. 30, pp. 614-627
- [11] A. Luque et al., 2008. Positive and negative streamers in ambient air: modeling evolution and velocities. *J. Phys. D: Appl. Phys.*, vol. 41, no. 234005

- [12] N. Liu et al., 2012. Formation of streamer discharges from an isolated ionization column at subbreakdown conditions. *Phys. Rev. Lett.*, vol. 109, 025002
- [13] J. Qin and V.P. Pasko, 2014. On the propagation of streamers in electrical discharges. *J. Phys. D: Appl. Phys.*, vol. 47, no. 435202
- [14] C.T. Russell, T.L. Zhang, M. Delva, W. Magnes, R.J. Strangeway, H.Y. Wei, 2007. Lightning on Venus inferred from whistler-mode waves in the ionosphere. *Nature*, vol. 450, pp. 661–662
- [15] Y. Takahashi, J. Yoshida, Y. Yair, T. Imamura and M. Nakamura, 2008. Lightning Detection by LAC Onboard the Japanese Venus Climate Orbiter, Planet-C. *Space Sci. Rev.*, vol. 137, pp. 317–334
- [16] A.C. Moinelo, S. Abildgaard, A.G. Muñoz, G. Piccioni and D. Grassi, 2016. No statistical evidence of lightning in Venus night-side atmosphere from VIRTIS-Venus Express Visible observations. *Icarus*, vol. 277, pp. 395–400
- [17] F.J. Pérez-Invernó, A. Luque and F.J. Gordillo-Vázquez, 2016. Mesospheric optical signatures of possible lightning on Venus. *J. Geophys. Res. Space Phys.*, vol. 121, pp. 7026–7048
- [18] A.R. Vasavada and A.P. Showman, 2005. Jovian atmospheric dynamics: an update after Galileo and Cassini. *Rep. Prog. Phys.*, vol. 68, pp. 1935–1996
- [19] Y. Yair, G. Fischer, F. Simoes, N. Renno and P. Zarka, 2008. Updated Review of Planetary Atmospheric Electricity. *Space Sci. Rev.*, vol. 137, pp. 29–49
- [20] U.A. Dyudina, A.P. Ingersoll, S.P. Ewald, C.C. Porco, G. Fischer, W.S. Kurth and R.A. West, 2010. Detection of visible lightning on Saturn. *Geophys. Res. Lett.*, vol. 37, L09205
- [21] U.A. Dyudina, A.P. Ingersoll, S.P. Ewald, C.C. Porco, G. Fischer and Y. Yair, 2013. Saturn's visible lightning, its radio emissions, and the structure of the 2009-2011 lightning storms. *Icarus*, vol. 226, pp. 1020–1037
- [22] G. Fischer, D.A. Gurnett, W.S. Kurth, F. Akalin, P. Zarka, U.A. Dyudina, W. M. Farrell and M.L. Kaiser, 2008. Atmospheric Electricity at Saturn. *Space Sci. Rev.*, vol. 137, pp. 271–285

- [23] P. Zarka and B.M. Pedersen, 1986. Radio detection of uranian lightning by Voyager 2. *Nature*, vol. 323, pp. 605–608
- [24] D.A. Gurnett, W. S Kurth, I.H. Cairns, L.J. Granroth, 1990. Whistlers in Neptune’s Magnetosphere: Evidence of Atmospheric Lightning. *J. Geophys. Res.*, vol. 95, pp. 20967–20976
- [25] S.G. Gibbard, E.H. Levy, J.I. Lunine and I. de Pater, 1999. Lightning on Neptune. *Icarus*, vol. 139, pp. 227–234
- [26] N.O. Renno, A.S. Wong, S.K. Atreya, I. de Pater and M. Roos-Serote, 2003. Electrical discharges and broadband radio emission by Martian dust devils and dust storms. *Geophys. Res. Lett.*, vol. 30, 2140
- [27] C. Ruf, N.O. Renno, J.F. Kok, E. Bandelier, M.J. Sander, S. Gross, L. Skjerve and B. Cantor, 2009. Emission of non-thermal microwave radiation by a Martian dust storm. *Geophys. Res. Lett.*, vol. 36, L13202
- [28] O. Melnik and M. Parrot, 1998. Electrostatic discharge in Martian dust storms. *J. Geophys. Res.*, vol. 103, pp. 29107–29117
- [29] M.M. Anderson, A.P.V. Siemion, W.C. Barott, G.C. Bower, G.T. Delory, I. de Pater and D. Werthimer, 2012. The Allen Telescope Array search for electrostatic discharges on Mars. *Astro. J.*, vol. 744:15
- [30] D.A. Gurnett, D.D. Morgan, L.J. Granroth, B.A. Cantor, W.M. Farrell and J.R. Espley, 2010. Non-detection of impulsive radio signals from lightning in Martian dust storms using the radar receiver on the Mars Express spacecraft. *Geophys. Res. Lett.*, vol. 37, L17802
- [31] J.R. Dwyer, L.M. Coleman, R. Lopez, Z. Saleh, D. Concha, M. Brown and H.K. Rassoul, 2006. Runaway breakdown in the Jovian atmospheres. *Geophys. Res. Lett.*, vol. 33, L22813
- [32] A.V. Gurevich, G.M. Milikh and R.A. Roussel-Dupré, 1992. Runaway electron mechanism of air breakdown and preconditioning during a thunderstorm. *Phys. Lett. A*, vol. 165, pp. 463–468
- [33] W.J. Borucki, R.L. Mc Kenzie, C.P. McKay, N.D. Duong and D.S. Boac, 1985. Spectra of simulated lightning on Venus, Jupiter, and Titan. *Icarus*, vol. 64, pp. 221-232

- [34] D. Dubrovin, S. Nijdam, E.M. van Veldhuizen, U. Ebert, Y. Yair and C. Price, 2010. Sprite discharges on Venus and Jupiter-like planets: A laboratory investigation. *J. Geophys. Res.*, vol. 115, A00E34
- [35] D.T. Hall, D.F. Strobel, P.D. Feldman, M.A. McGrath and H.A. Weaver, 1995. Detection of an oxygen atmosphere on Jupiter's moon Europa. *Nature*, vol. 373, pp. 677–679
- [36] F. Raulin, 2005. Exo-astrobiological aspects of Europa and Titan: from observations to speculations. *Space Sci. Rev.*, vol. 116, pp. 471–487
- [37] J.C. Loison, E. Hébrard, M. Dobrijevic, K.M. Hickson, F. Caralp, V. Hue, G. Gronoff, O. Venot and Y. Bénilan, 2015. The neutral photochemistry of nitriles, amines and imines in the atmosphere of Titan. *Icarus*, vol. 247, pp. 218–247
- [38] J.B.S. Haldane, 1929. The origin of life. *Rationalist Annual*
- [39] A.I. Oparin, 1938. The origin of life. Macmillan, New York
- [40] P. Ward and J. Kirschvink, 2015. A new history of life: the radical discoveries about the origins and evolution of life on earth. Bloomsbury Press
- [41] J.H. Waite Jr., D.T. Young, T.E. Cravens, A.J. Coates, F.J. Crary, B. Magee and J. Westlake, 2007. The process of Tholin formation in Titan's Upper Atmosphere. *Science.*, vol. 316, pp. 870–875
- [42] S.L. Miller, 1953. A production of amino acids under possible primitive earth conditions. *Science*, vol. 117, 3046
- [43] S.L. Miller and H.C. Urey, 1959. Organic compound synthesis on the Primitive Earth. *Science*, vol. 130, 3370
- [44] K. Plankensteiner et al., 2007. Discharge experiments simulating chemical evolution on the surface of Titan. *Icarus*, vol. 187, pp. 616–619
- [45] M.D. Desch and M.L. Kaiser, 1990. Upper limit set for level of lightning activity on Titan. *Nature*, vol. 343, pp. 442–444
- [46] V.A. Rakov and M.A. Uman, 2003. *Lightning: Physics and Effects*. Cambridge Univ. Press, New York

- [47] M. Fulchignoni et al., 2005. In situ measurements of the physical characteristics of Titan's environment. *Nature*, vol. 438, pp. 785–791
- [48] C. Béghin et al., 2009. New insights on Titan's plasma-driven Schumann resonance inferred from Huygens and Cassini data. *Planetary and Space Sci.*, vol. 57, pp. 1872–1888
- [49] H. Lammer, T. Tokano, G. Fischer, W. Stumtner, G.J. Molina-Cuberos, K. Schwingenschuh and H.O. Rucker, 2001. Lightning activity on Titan: can Cassini detect it? *Planetary Space Sci.*, vol. 49, pp. 561–574
- [50] G. Fischer, D.A. Gurnett, W.S. Kurth, W.M. Farrell, M.L. Kaiser and P. Zarka, 2007. Nondetection of Titan lightning radio emissions with Cassini/RPWS after 35 close Titan flybys. *Geophys. Res. Lett.*, vol. 34, L22104
- [51] R. Lorenz and J. Mitton, 2008. *Titan Unveiled*. Princeton University Press, New Jersey
- [52] G. Fischer and D.A. Gurnett, 2011. The search for Titan lightning radio emissions. *Geophys. Res. Lett.*, vol. 38, L08206
- [53] A. Bar-Nun and M. Podolak, 1979. The photochemistry of hydrocarbons in Titan's atmosphere. *Icarus*, vol. 38, pp. 115–122
- [54] W.J. Borucki, L.P. Giver, C.P. McKay, T. Scattergood and J.E. Pariss, 1988. Lightning production of hydrocarbons and HCN on Titan: laboratory measurements. *Icarus*, vol. 76, pp. 125–134
- [55] F.W. Taylor and A. Coustenis, 1998. Titan in the solar system. *Planet Space Sci.*, vol. 46, pp. 1085–1097
- [56] L. Wåhlin, 1994. Elements of fair weather electricity. *J. Geophys. Res.*, vol. 99, pp. 10767–10772
- [57] G.J. Molina-Cuberos, J.J. López-Moreno, R. Rodrigo and K. Schwingenschuh, 2001. Capability of the Cassini/Huygens PWA-HASI to measure electrical conductivity in Titan. *Adv. Space Res.*, vol. 28, pp. 1511–1516
- [58] T. Tokano, G.J. Molina-Cuberos, H. Lammer and W. Stumtner, 2001. Modelling of thunderclouds and lightning generation on Titan. *Planetary and Space Sci.*, vol. 49, pp. 539–560

- [59] O. Chanrion and T. Neubert, 2008. A PIC-MCC code for simulation of streamer propagation in air. *J. Comp. Phys.*, vol. 227, pp. 7222-7245
- [60] O. Chanrion and T. Neubert, 2010. Production of runaway electrons by negative streamer discharges. *J. Geophys. Res.*, vol. 115, A00E32
- [61] A.V. Gurevich, 1961. On the theory of runaway electrons. *Sov. Phys. JETP*, vol. 12, pp. 904–912
- [62] A.V. Phelps and L.C. Pitchford, 1985. Anisotropic scattering of electrons by  $N_2$  and its effect on electron transport. *Phys. Rev. A*, vol. 31, pp. 2932–2949
- [63] R. Crompton, 1994. Benchmark measurements of cross sections for electron collisions: electron swarm methods. *Adv. Atom., Molecular Opt. Phys.*, vol. 32, pp. 97–148
- [64] G.D. Moss, V.P. Pasko, N. Liu and G. Veronis, 2006. Monte Carlo model for analysis of thermal runaway electrons in streamer tips in transient luminous events and streamer zones of lightning leaders. *J. Geophys. Res.*, vol. 111, A20307
- [65] S. Dujko, U. Ebert, R.D. White and Z. Lj. Petrović, 2011. Boltzmann Equation Analysis of Electron Transport in a  $N_2$ - $O_2$  Streamer Discharge, 2011. *Jpn. J. Appl. Phys.*, vol. 50, 08JC01
- [66] C. Li, U. Ebert and W. Hundsdorfer, 2012. Spatially hybrid computations for streamer discharges: II. Fully 3D simulations. *J. Comp. Phys.*, vol. 231, pp. 1020–1050
- [67] C. Köhn and U. Ebert, 2014. The structure of ionization showers in air generated by electrons with 1 MeV energy or less. *Plasma Sour. Sci. Technol.*, vol. 23, 045001
- [68] C. Köhn and U. Ebert, 2015. Calculation of beam of positrons, neutrons and protons associated with terrestrial gamma-ray flashes. *J. Geophys. Res. Atmos.*, vol. 120, pp. 1620–1635
- [69] C. Köhn, O. Chanrion and T. Neubert, 2017. The influence of bremsstrahlung on electric discharge streamers in  $N_2$ ,  $O_2$  gas mixtures. *Plasma Sour. Sci. Technol.*, vol. 26, 015006

- [70] M. Arrayás, U. Ebert and W. Hundsdorfer, 2002. Spontaneous branching of anode-directed streamers between planar electrodes. *Phys. Rev. Lett.*, vol. 88, 174502
- [71] N. Liu and V.P. Pasko, 2004. Effects of photoionization on propagation and branching of positive and negative streamers in sprites. *J. Geophys. Res.*, vol. 109, A04301
- [72] H.B. Niemann et al., 2005. The abundances of constituents of Titan's atmosphere from the GCMS instrument on the Huygens probe. *Nature*, vol. 438, pp. 779–784
- [73] G.F. Lindal, G.E. Wood, H.B. Hotz, D.N. Sweetnam, V.R. Eshleman and G.L. Tyler, 1983. The Atmosphere of Titan: An Analysis of the Voyager 1 Radio Occultation Measurements. *Icarus*, vol. 53, pp. 348–363
- [74] C.P. McKay, J.B. Pollack and R. Courtin, 1989. The thermal structure of Titan's atmosphere. *Icarus*, vol. 80, pp. 23–53
- [75] E.L. Barth and S.C.R. Rafkin, 2007. TRAMS: A new dynamic cloud model for Titan's methane clouds. *Geophys. Res. Lett.*, vol. 34, L03203
- [76] C.A. Griffith et al., 2009. Characterization of clouds in Titan's tropical atmosphere. *Astro. J.*, vol. 702, L105–L109
- [77] I. Müller-Wodrag, C.A. Griffith, E. Lellouch and T.E. Cravens, 2014. Titan: Interior, Surface, Atmosphere, and Space Environment. Cambridge University Press, New York
- [78] O. Šašić, G. Malović, A. Strinić, Ž. Nikitović and Z. Lj. Petrović, 2004. Excitation coefficients and cross-sections for electron swarms in methane. *New. J. of Phys.*, vol. 6, 74
- [79] C. Li, 2009. Joining particle and fluid aspects in streamer simulations. PhD thesis. Technical University of Eindhoven, DOI:10.6100/IR640104
- [80] S. Celestin and V.P. Pasko, 2010. Soft collisions in relativistic runaway electron avalanches. *J. Phys. D: Appl. Phys.*, vol. 43, 315206
- [81] M.B. Zheleznyak et al., 1982. Photoionization of nitrogen and oxygen mixtures from a gas discharge. *High Temp.*, vol. 20, pp. 357-362

- [82] A. Luque et al., 2007. Photoionization in negative streamers: Fast computations and two propagation modes. *Appl. Phys. Lett.*, vol. 90, 081501
- [83] A. Bourdon et al., 2007. Efficient models for photoionization produced by non-thermal gas discharges in air based on radiative transfer and the Helmholtz equations. *Plasma Sour. Sc. Tech.*, vol. 16, pp. 656-678
- [84] G. Wormeester et al., 2010. Probing photo-ionization: simulations of positive streamers in varying  $N_2:O_2$ -mixtures. *J. Phys. D: Appl. Phys.*, vol. 43, 505201
- [85] S. Pancheshnyi, 2005. Role of electronegative gas admixtures in streamer start, propagation and branching phenomena. *Plasma Sour. Sci. Technol.*, vol. 14, pp. 645–653
- [86] S. Nijdam et al., 2011. Probing background ionization: positive streamers with varying pulse repetition rate and with a radioactive admixture. *J. Phys. D: Appl. Phys.*, vol. 44, 455201
- [87] V.L. Carter, 1972. HighResolution  $N_2$  Absorption Study from 730 to 980 Å. *J. Chem. Phys.*, vol. 56, pp. 4195–4205
- [88] Y.P. Raizer, 1991. *Gas Discharge Physics*. Berlin, Springer
- [89] D. Bošnjaković, I. Simonović, Z.Lj. Petrović, C. Köhn and S. Dujko, 2018. Electron transport and propagation of negative planar ionization fronts in  $N_2:CH_4$ -mixtures. Manuscript submitted to *Plasma Sour. Sci. Technol.*
- [90] T.C. Marshall, M.P. McCarthy and W.D. Rust, 1995. Electric field magnitudes and lightning initiation in thunderstorms. *J. Geophys. Res.*, vol. 100, pp. 7097–7103
- [91] T.C. Marshall, M. Stolzenburg, C.R. Maggio, L.M. Coleman, P.R. Krehbiel, T. Hamlin, R.J. Thomas and W. Rison, 2005. Observed electric fields associated with lightning initiation. *Geophys. Res. Lett.*, vol. 32, L03813
- [92] A.V. Gurevich and A.N. Karashtin, 2013. Runaway breakdown in hydrometeors in lightning initiation. *Phys. Rev. Lett.*, vol. 110, 185005

- [93] A. Dubinova, C. Rutjes, U. Ebert, S. Buitink, O. Scholten and G.T.N. Trinh, 2015. Prediction of lightning inception by large ice particles and extensive air showers. *Phys. Rev. Lett.*, vol. 115, 015002
- [94] G. Fischer. Personal communication, 2018
- [95] R.L. Bailey, C. Helling, G. Hodosán, C. Bilger and C.R. Stark, 2014. Ionization in Atmospheres of Brown Dwarfs and Extrasolar Planets VI: Properties of Large-scale discharge Events. *Astro. J.*, vol. 784, 43
- [96] G. Hodosán, C. Helling, R. Asensio-Torres, I. Vorgul and P.B. Rimmer, 2016. Lightning climatology of exoplanets and brown dwarfs guided by Solar system data. *Monthly Not. Royal Astro. Soc.*, vol. 461, pp. 3927–3947
- [97] G. Hodosán, P.B. Rimmer and C. Helling, 2016. Is lightning a possible source of the radio emission on HAT-P\_11b. *Monthly Not. Royal Astro. Soc.*, vol. 461, pp. 1222–1226